ACS APPLIED MATERIALS & INTERFACES

Research Article

www.acsami.org

Mechanochemically Active Soft Robots

Gregory R. Gossweiler, Cameron L. Brown, Gihan B. Hewage, Eitan Sapiro-Gheiler, William J. Trautman, Garrett W. Welshofer, and Stephen L. Craig*

Department of Chemistry, Duke University, Durham, North Carolina 27708, United States

Supporting Information

ABSTRACT: The functions of soft robotics are intimately tied to their form—channels and voids defined by an elastomeric superstructure that reversibly stores and releases mechanical energy to change shape, grip objects, and achieve complex motions. Here, we demonstrate that covalent polymer mechanochemistry provides a viable mechanism to convert the same mechanical potential energy used for actuation in soft robots into a mechanochromic, covalent chemical response. A bis-alkene functionalized spiropyran (SP) mechanophore is cured into a molded poly(dimethylsiloxane) (PDMS) soft robot walker and gripper. The stresses and strains necessary for SP activation are compatible with soft robot function. The color change associated with actuation suggests opportunities for not only new color changing or camouflaging strategies, but also the possibility for simultaneous activation of latent chemistry (e.g., release of small molecules, change in mechanical properties, activation of catalysts, etc.) in soft robots. In addition, mechanochromic stress mapping in a functional robotic device might provide a useful design and optimization tool, revealing spatial and temporal force evolution within the robot in a way that might be coupled to autonomous feedback loops that allow the robot to regulate its own activity. The demonstration motivates the simultaneous development of new combinations of mechanophores, materials, and soft, active devices for enhanced functionality.

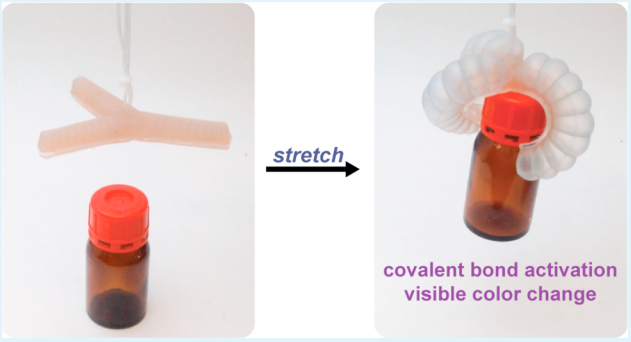

KEYWORDS: *mechanochemistry, soft robot, spiropyran, PDMS, stimuli-responsive, mechanochromic*

INTRODUCTION

Recent work in soft robotics has inspired a fleet of new demonstrated capabilities, including starfish-,[1,2] tentacle-,[2,3] and human-hand-like[4,5] locomotion;[4,6,7] high-strength composite structures;[8,9] electrical components;[3,4] a heartlike pump;[10] and camouflage.[11] All of these functions have been realized using relatively inexpensive and widely accessible materials. In contrast to traditional "hard" robots, soft robots are fabricated from mechanically soft and flexible elastomers. Pneumatic or hydraulic inflation of elastomeric channels and voids produces the remarkably complex and nonlinear macroscopic motions of soft robots. Underlying the macroscopic curls, twists, and undulations of the soft robot, there exist associated molecular deformations. The "macroscopic-to-molecular" connection involved in force transmission provides an opportunity to use the material as a multipurpose actuator; on the one hand, the inflation of channels and voids drives the macroscopic actuation and locomotion traditionally associated with robotics, while, on the other, the network simultaneously channels macroscopic tension to discrete network-bound mechanophores (Figure 1), converting mechanical potential to covalent chemical response. The nature of the mechanophore can be selected from a growing menu of options, which to date includes small molecule release[12−14] and acid generation,[15] covalent bond scission leading to color change,[14,16−21] luminescence,[22,23] repair and stress toughening,[24] and catalysis.[25,26] The addition of mechanochemical activity therefore has the potential to enrich soft robotics with changes in physical and/or chemical properties upon actuation that are similar to mechanisms widespread in nature (e.g., camouflage, toxin release, damage sensing and repair, and chemical signaling).

We recently demonstrated a first generation mechanochemical device, in which electroactive elastomeric films are coupled to mechanochemical activation to create soft displays that simultaneously change surface topography, color, and fluorescence in response to a remote electric potential.[27] Here, we extend our studies of mechanochemically active soft devices to silicone elastomer-based soft robots. The methodology exploits the platinum catalyzed hydrosilylation cure chemistry found in most commercial silicone kits (e.g., Smooth-On Ecoflex) to easily incorporate a mechanophore into the covalent network of the elastomer. Following our earlier work on electromechanochemically active displays, we demonstrate the concept using the spiropyran mechanophore developed by Sottos, Moore, and co-workers.[16] In response to sufficient molecular tension (on the order of 200 pN for activation on the

Received: July 17, 2015
Accepted: September 21, 2015
Published: September 21, 2015

ACS Publications © 2015 American Chemical Society

DOI: 10.1021/acsami.5b06440
ACS Appl. Mater. Interfaces 2015, 7, 22431−22435

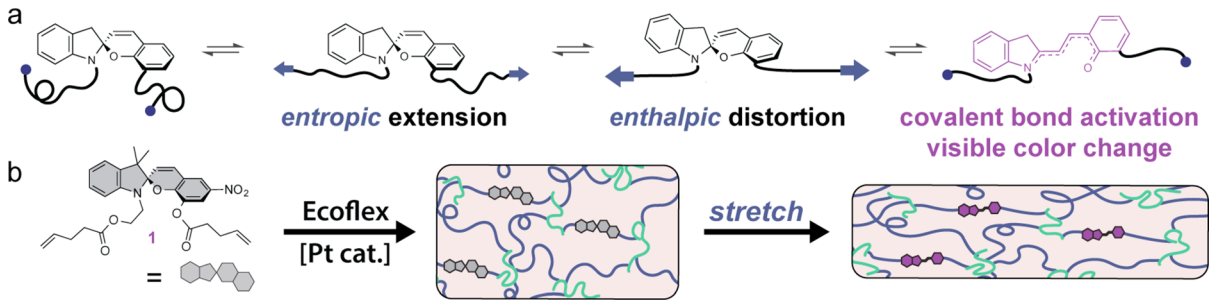

Figure 1. Schematic diagram of the mechanochemical energy transduction hierarchy used here. (a) The mechanochemical response of a spiropyran mechanophore is coupled to mechanical deformation of polymer subchains that increase with force. (b) When a bis-functional spiropyran force-probe (**1**) is covalently bound to the network, macroscopic deformation couples into the same molecular deformations in (a), producing macroscopically observable coloration and fluorescence.

time scale of seconds[28]), spiropyran undergoes a unimolecular reaction to its extended and conjugated merocyanine form (Figure 1a).[16] The product merocyanine provides a visible color change and gives rise to a measurable change in fluorescence. SP activation occurs in areas where the local strain is highest and, in the context of soft robotics, provides a useful indication of stresses and strains experienced by the robot during operation. The response therefore creates not only a potential camouflaging mechanism, it might also aid in failure detection and analysis and design optimization.

We focused our initial efforts on pneumatically driven soft robots. The same platinum catalyzed hydrosilylation reaction that cures the Ecoflex also incorporates the spiropyran mechanophore into the network (Figure 1b), leading to a mechanochemically active Ecoflex polymer that is analogous to prior work in Sylgard 184.[14] The actuation involves biaxial extension associated with inflation, and so we first assessed mechanophore activation in simple Ecoflex "balloons." On the first inflation, the onset of an observable color change occurs at a biaxial stretch of $\varepsilon \sim 0.7$. Deflation leads to about 95% shape recovery and the mechanically triggered color change recedes to its initial coloration after approximately 10 min (see Figure S7). Repeating the inflation (Figure 2b) leads to a second mechanically induced color change that is somewhat less pronounced than the first (presumably because of hysteresis associated with the well-known Mullins effect[29−31]). Subsequent cycles (Figure 2e) have good reproducibility. Thus, spiropyran-linked Ecoflex seemed to meet the criteria for use in mechanochemically active soft robots.

We therefore constructed two types of soft robot to test whether the mechanochemical covalent response was compatible with some standard robot designs and actuation. Shown in Figure 3 are a three-arm gripper and a five-arm walker. The molds and dimensions of each robot are provided in the Supporting Information. As seen in Figure 3, pneumatic actuation of each type of device leads to gripping motions (Figure 3a and sequential inflation of legs for walking (Figure 3b, 1−6) that not only provide the desired motions, but also lead to color change through the desired covalent chemical reaction. The robots recover their initial form when the actuating pressure is removed and maintain the color change for approximately 10 min, as observed in the model balloon geometry discussed above.

We note that neither the mechanical device performance nor the mechanochromic response is optimized; rather, these demonstrations serve as proof-of-principle for the compatibility of blending the two functions in soft robots. Entirely different

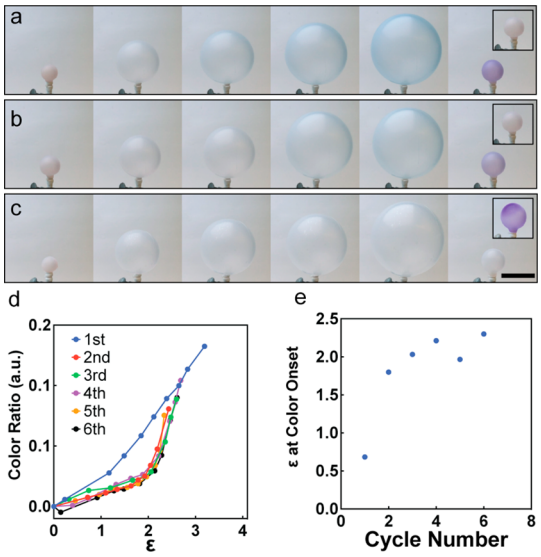

Figure 2. Inflation of a spiropyran-containing balloon reveals a color change that persists for several minutes when the balloon is relaxed (a), but returns upon subsequent inflation (b). Images of the balloon after 10 min at rest are shown (a, b, inset images). A mechanically inactive control balloon does not show the characteristic color change upon inflation (c). UV irradiation of the balloon produces the characteristic color change, confirming the presence of the molecule (c, inset). The color intensity can be tracked with a traditional digital color camera, and is shown as an increase in red color channel intensities, where ratio = R/(R + G + B) (d). The characteristic strain of color onset is shown, plotted against the number of repeated inflation cycles (e). $\varepsilon = (r - r_{initial})/r_{initial}$ (see the Supporting Information for additional details and full images with color card). Scale bar = 7 cm. Photos taken over ∼30 s, but no substantial time dependence is observed (see Figure S12).

device architectures might be engineered in the future, depending on the relative importance of the physical function relative to maximizing color change or camouflage. But the stress-responsive mechanochromism might serve other important functions as well. For example, we wondered if the location of most intense response might serve as an indication of the region of most probable failure. To test that idea, we fabricated the three-arm gripper shown in Figure 4a. Inflation of the gripper led to the greatest color change at the figurative knuckles of the device, but the arms did not experience identical levels of mechanochromism. Contrast can be further enhanced via macroscopic fluorescence imaging of the activated merocyanine, conducted here by exciting the activated

DOI: 10.1021/acsami.5b06440
ACS Appl. Mater. Interfaces 2015, 7, 22431−22435

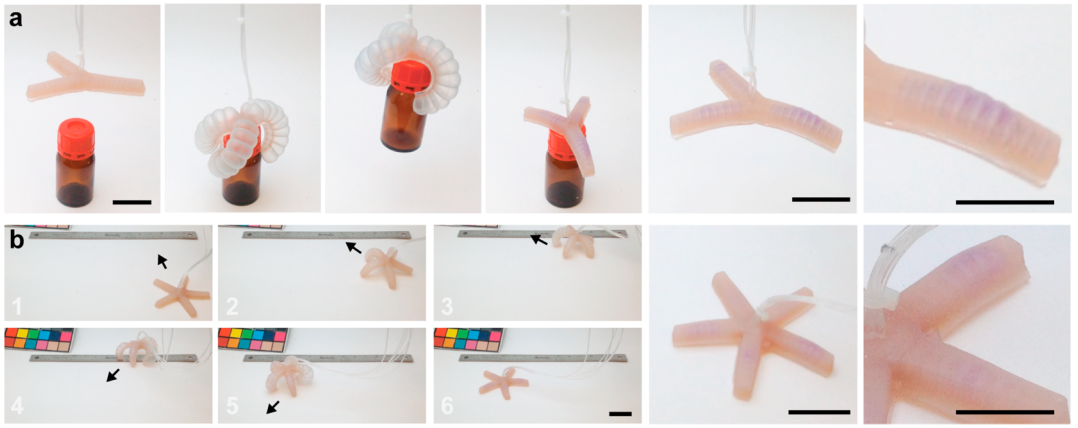

Figure 3. Three-arm gripping robot (a) and five-arm walking robot (b) are shown. Initial robots (left) are inflated to produce a color change when network stresses/strains reach a critical value. The color persists for several minutes after the robot is returned to the initial state (right). The inset numbers indicate the temporal order of the images. Scale bars = 5 cm.

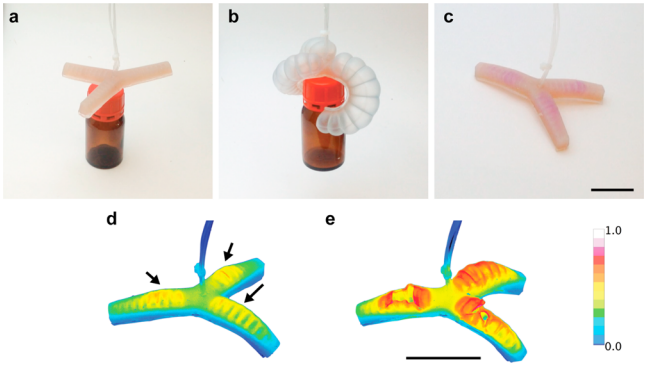

Figure 4. Inflation of a three-arm gripper robot reveals more intense coloration in regions that experience the largest deformations. Shown are color images before (a), during (b), and after (c) inflation of the gripper. (d) Fluorescent images of the robot after the deformation with arrows indicating the "at-risk" regions. Overinflation of the robot until rupture validates that the indicated regions are "at-risk" of failure (e). Scale bars = 5 cm.

merocyanine with diffuse green LED light within a rudimentary "dark room" while imaging through a long-pass filter (additional details in the Supporting Information). The fluorescent images reveal localized regions of greater intensity on each arm (indicated by the arrows in Figures 4d) in both visible color change and differential fluorescence. That initial color change obtained in the reversible actuation response of the gripper was predictive of failure, as subsequent overinflation led to rupture in the soft robot at the position of prior, highest mechanochemical response.

Finally, the mechanochemical activity can be used to provide a mechanism by which a soft robot can sense and report on its past physical environment. When a robot is inflated beyond the capacity of a confined space, the external confinement will disrupt the growing shape of the inflating robot, leading to a perturbation of the stresses and strains experienced within the robot. This concept is demonstrated in Figure 5. Inflating a sphere within a room whose walls are pillared generates a mechanochemical, colorimetric imprint of the surrounding on the surface of the robot.

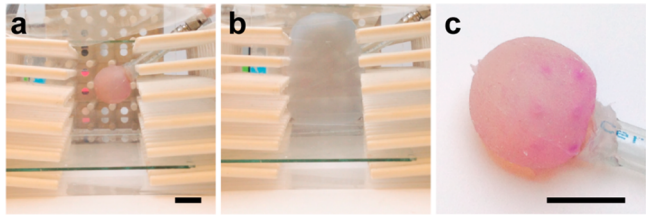

Figure 5. Sphere that inflates and has memory of its container. (a) Initial sphere. (b) Inflation within a "room" with pillars on the walls leads to colored demarcations that are determined by the topological constraints of the space (c). Note that (c) is magnified to make the contrast more visible. Scale bars = 2 cm.

CONCLUSIONS

The demonstrations provided here show that soft robot actuation and covalent mechanochemical response are compatible within the same devices, in that mechanochemical activation accompanies reversible and repeatable soft robot actuation. The fact that the two go more or less hand-in-hand in these demonstrations is encouraging, as the Ecoflex platform chosen is one that was originally developed because it works well for only the purpose of mechanical actuation. Future improvements should be realized by optimizing the material for the dual purposes of mechanical and molecular actuation shown here.

While the levels of mechanochromism reported here might be suitable for a selected set of color-changing or camouflaging applications, functional mechanochromism in most cases will likely require both the development of mechanophores with task-specific "resting" and "active" coloration, as well device designs that optimize the intensity and distribution of the mechanochromism in concert with the mechanical function of the soft robots. Mechanochromism is not the only desirable covalent chemical response, however, and one can envision potential applications in which the release of small molecules[12,14] or activation of a catalyst[25,32] might be desirable functions to blend into active, soft robotic devices. Covalent polymer mechanochemistry has also been used to trigger cross-linking reactions in response to otherwise destructive forces,[24] and the ability to create self-healing behavior in autonomous soft robots has been noted to be an especially attractive goal, given susceptibility of soft robots to mechanical damage.[9,33,34]

DOI: 10.1021/acsami.5b06440
ACS Appl. Mater. Interfaces 2015, 7, 22431−22435

While many of these responses might currently be more challenging to realize in PDMS elastomers than spiropyran activation, we note that in at least two cases (perturbed catalysis[35] and retro-cycloaddition[14]) the requirements for activation appear to be quite similar to those for spiropyran.

Along those lines, the potential to sense stress concentrations and identify at-risk regions for eventual failure might provide a useful tool for not only optimizing soft robot design, but also for streamlining their maintenance. PDMS-based soft robots are an inexpensive and high-throughput technology that enables design, fabrication, and testing of a prototype in the span of hours. Multiple iterations of redesign and fabrication to arrive at the intended function are typically done empirically and intuitively.[1] Modeling has been used to improve designs from an understanding of the structure−property relationships.[1,3,4,36,37] Unlike hard robots, the nonlinear mechanical properties of a fully fabricated soft robot are difficult to consistently reproduce and anticipate in FEA software, especially when comparing an idealized model to the as-fabricated design. Incorporating a probe within the material provides a simple and general method to get real-time information on stress-concentration during normal operation, and up to failure, in addition to the absence of stress-concentration, which is equally as informative.

This latter capability is better regarding as a means of data acquisition and reporting, effectively a mechanism for input rather than functional output. The demonstration of mechanochemical imprinting suggests a similar opportunity, but in this case to probe and report on external physical environment rather than internal mechanical state. This form of metrology is similar to that demonstrated recently in mechanochemical "scales" that assess the weight of an attached object.[21] While other methods for these types of measurements already exist, the ability to incorporate them directly into the functional material component of the device, as well as the simple visual readout, has some obvious advantages in fabrication. As mechanophore design moves from proof-of-concept demonstrations to implementation as functional components in materials and devices, we therefore imagine that soft robots will join other device and material platforms as a target that generates its own set of tailored mechanophores optimized for that purpose.

METHODS

Design and Fabrication. Soft robot molds were designed in Autodesk Inventor (San Rafael, CA) and were 3D printed via fused deposition modeling on either a Replicator 2X 3D Printer (Makerbot, New York, NY) or Lulzbot Mini (Lulzbot Loveland, CO) from natural/color-free ABS filament purchased from the printer manufacturer. The printed molds were then filed to smooth edges and to remove any overprint. A bis-alkene derivative of the mechanochromic molecule spiropyran[14] (**1**, Figure 1) was incorporated into Ecoflex (Smooth-On, Macungie, PA) as follows. Ecoflex 10−30 prepolymer in a 1:1 ratio of part A:B was thoroughly mixed with a solution of spiropyran (0.2% w/w) in diethyl ether (10% v/w), and the entire mixture was degassed for 1 min (35 Torr) before pouring into the ABS molds. The robots were cured for 2−3 h at 60 °C and were promptly demolded. Fabrication of the mechanically inactive control balloons followed an identical procedure, substituting only the spiropyran molecule, as reported previously.[14] The 3-arm and 5-arm robots were sealed to Sylgard 184 substrates (2−3 mm thickness) with Sil-Poxy silicone adhesive (Smooth-On, Macungie, PA). Individual channel control was achieved through the use of several push-button style miniature air directional control valves (McMaster-Carr, part # 62475K12).

Macroscopic Fluorescence Analysis. To obtain fluorescence images of the robots, a "dark" room was created out of PVC pipe and general purpose black-out curtains. Within the dark room was mounted a 36 W RGB LED light panel (www.superbrightLEDs.com, individual color LED emission maxima centered at 466, 522, and 633 nm). For the fluorescence test, the red LEDs were disabled and the green and blue LED provided the sole source of illumination (spectral emission curves can be found in the Supporting Information). Images were captured with a Canon EOS Rebel XSi camera with a 610 nm Thorlabs long-pass color filter mounted between the camera and the robot. Raw images were processed in ImageJ/Fiji to remove background and to apply the 16-color LUT.

ASSOCIATED CONTENT

Supporting Information

The Supporting Information is available free of charge on the ACS Publications website at DOI: 10.1021/acsami.5b06440.

Fabrication procedures, additional details, and raw images (PDF)
Video of three-arm gripping robot (AVI)
Video of five-arm walking robot (AVI)

AUTHOR INFORMATION

Corresponding Author

*E-mail: stephen.craig@duke.edu.

Author Contributions

G.B.H. and G.W.W. conceived the initial idea. All authors save S.L.C. designed, manufactured, and tested various soft robots. G.R.G. did the image analysis. G.R.G. and S.L.C. wrote the manuscript. All authors have given approval to the final version of the manuscript.

Funding

This material is based on work supported by NSF through the Research Triangle MRSEC (DMR-1121107). G.W.W. and G.B.H. were supported by summer fellowships from the NSF (CHE-1062607) and Duke University, respectively

Notes

The authors declare no competing financial interest.

ACKNOWLEDGMENTS

We thank X. Zhao, S. Lin, and S. Hong for access to their 3D printers.

ABBREVIATIONS

SP, spiropyran; PDMS, poly(dimethylsiloxane); FEA, Finite Element Analysis

REFERENCES

(1) Ilievski, F.; Mazzeo, A. D.; Shepherd, R. F.; Chen, X.; Whitesides, G. M. Soft Robotics for Chemists. *Angew. Chem., Int. Ed.* **2011**, *50*, 1890−1895.

(2) Kwok, S. W.; Morin, S. A.; Mosadegh, B.; So, J. H.; Shepherd, R. F.; Martinez, R. V.; Smith, B.; Simeone, F. C.; Stokes, A. A.; Whitesides, G. M. Magnetic Assembly of Soft Robots with Hard Components. *Adv. Funct. Mater.* **2014**, *24*, 2180−2187.

(3) Martinez, R. V.; Branch, J. L.; Fish, C. R.; Jin, L.; Shepherd, R. F.; Nunes, R. M.; Suo, Z.; Whitesides, G. M. Robotic Tentacles with Three-Dimensional Mobility Based on Flexible Elastomers. *Adv. Mater.* **2013**, *25*, 205−212.

(4) Polygerinos, P.; Lyne, S.; Wang, Z.; Nicolini, L. F.; Mosadegh, B.; Whitesides, G. M.; Walsh, C. J. Towards a Soft Pneumatic Glove for Hand Rehabilitation. *Intelligent Robots and Systems (IROS)* **2013**, 1512−1517.

DOI: 10.1021/acsami.5b06440
ACS Appl. Mater. Interfaces 2015, 7, 22431−22435

(5) Deimel, R.; Brock, O. A Novel Type of Compliant and Underactuated Robotic Hand for Dexterous Grasping. *Robot: Sci. Syst.* **2014**, 1687−1692.
(6) Shepherd, R. F.; Ilievski, F.; Choi, W.; Morin, S. A.; Stokes, A. A.; Mazzeo, A. D.; Chen, X.; Wang, M.; Whitesides, G. M. Multigait Soft Robot. *Proc. Natl. Acad. Sci. U. S. A.* **2011**, *108*, 20400−20403.
(7) Shepherd, R. F.; Stokes, A. A.; Freake, J.; Barber, J.; Snyder, P. W.; Mazzeo, A. D.; Cademartiri, L.; Morin, S. A.; Whitesides, G. M. Using Explosions to Power a Soft Robot. *Angew. Chem., Int. Ed.* **2013**, *52*, 2892−2896.
(8) Martinez, R. V.; Fish, C. R.; Chen, X.; Whitesides, G. M. Elastomeric Origami: Programmable Paper-Elastomer Composites as Pneumatic Actuators. *Adv. Funct. Mater.* **2012**, *22*, 1376−1384.
(9) Shepherd, R. F.; Stokes, A. A.; Nunes, R. M.; Whitesides, G. M. Soft Machines That are Resistant to Puncture and That Self Seal. *Adv. Mater.* **2013**, *25*, 6709−6713.
(10) Roche, E. T.; Wohlfarth, R.; Overvelde, J. T.; Vasilyev, N. V.; Pigula, F. A.; Mooney, D. J.; Bertoldi, K.; Walsh, C. J. A Bioinspired Soft Actuated Material. *Adv. Mater.* **2014**, *26*, 1200−1206.
(11) Morin, S. A.; Shepherd, R. F.; Kwok, S. W.; Stokes, A. A.; Nemiroski, A.; Whitesides, G. M. Camouflage and Display for Soft Machines. *Science* **2012**, *337*, 828−832.
(12) Larsen, M. B.; Boydston, A. J. "Flex-activated" Mechanophores: Using Polymer Mechanochemistry to Direct Bond Bending Activation. *J. Am. Chem. Soc.* **2013**, *135*, 8189−8192.
(13) Larsen, M. B.; Boydston, A. J. Successive Mechanochemical Activation and Small Molecule Release in an Elastomeric Material. *J. Am. Chem. Soc.* **2014**, *136*, 1276−1279.
(14) Gossweiler, G. R.; Hewage, G. B.; Soriano, G.; Wang, Q. M.; Welshofer, G. W.; Zhao, X. H.; Craig, S. L. Mechanochemical Activation of Covalent Bonds in Polymers with Full and Repeatable Macroscopic Shape Recovery. *ACS Macro Lett.* **2014**, *3*, 216−219.
(15) Diesendruck, C. E.; Steinberg, B. D.; Sugai, N.; Silberstein, M. N.; Sottos, N. R.; White, S. R.; Braun, P. V.; Moore, J. S. Proton-Coupled Mechanochemical Transduction: A Mechanogenerated Acid. *J. Am. Chem. Soc.* **2012**, *134*, 12446−12449.
(16) Davis, D. A.; Hamilton, A.; Yang, J.; Cremar, L. D.; Van Gough, D.; Potisek, S. L.; Ong, M. T.; Braun, P. V.; Martinez, T. J.; White, S. R.; Moore, J. S.; Sottos, N. R. Force-Induced Activation of Covalent Bonds in Mechanoresponsive Polymeric Materials. *Nature* **2009**, *459*, 68−72.
(17) O'Bryan, G.; Wong, B. M.; McElhanon, J. R. Stress Sensing in Polycaprolactone Films via an Embedded Photochromic Compound. *ACS Appl. Mater. Interfaces* **2010**, *2*, 1594−1600.
(18) Fang, X. L.; Zhang, H.; Chen, Y. J.; Lin, Y. J.; Xu, Y. Z.; Weng, W. G. Biomimetic Modular Polymer with Tough and Stress Sensing Properties. *Macromolecules* **2013**, *46*, 6566−6574.
(19) Lee, C. K.; Davis, D. A.; White, S. R.; Moore, J. S.; Sottos, N. R.; Braun, P. V. Force-Induced Redistribution of a Chemical Equilibrium. *J. Am. Chem. Soc.* **2010**, *132*, 16107−16111.
(20) Hemmer, J. R.; Smith, P. D.; van Horn, M.; Alnemrat, S.; Mason, B. P.; de Alaniz, J. R.; Osswald, S.; Hooper, J. P. High Strain-Rate Response of Spiropyran Mechanophores in PMMA. *J. Polym. Sci., Part B: Polym. Phys.* **2014**, *52*, 1347−1356.
(21) Peterson, G. I.; Larsen, M. B.; Ganter, M. A.; Storti, D. W.; Boydston, A. J. 3D-Printed Mechanochromic Materials. *ACS Appl. Mater. Interfaces* **2015**, *7*, 577−583.
(22) Chen, Y.; Spiering, A. J.; Karthikeyan, S.; Peters, G. W.; Meijer, E. W.; Sijbesma, R. P. Mechanically Induced Chemiluminescence from Polymers Incorporating a 1,2-Dioxetane Unit in the Main Chain. *Nat. Chem.* **2012**, *4*, 559−562.
(23) Ducrot, E.; Chen, Y.; Bulters, M.; Sijbesma, R. P.; Creton, C. Toughening Elastomers with Sacrificial Bonds and Watching Them Break. *Science* **2014**, *344*, 186−189.
(24) Ramirez, A. L. B.; Kean, Z. S.; Orlicki, J. A.; Champhekar, M.; Elsakr, S. M.; Krause, W. E.; Craig, S. L. Mechanochemical Strengthening of a Synthetic Polymer in Response to Typically Destructive Shear Forces. *Nat. Chem.* **2013**, *5*, 757−761.
(25) Piermattei, A.; Karthikeyan, S.; Sijbesma, R. P. Activating Catalysts with Mechanical Force. *Nat. Chem.* **2009**, *1*, 133−137.
(26) Groote, R.; Jakobs, R. T. M.; Sijbesma, R. P. Performance of Mechanochemically Activated Catalysts Is Enhanced by Suppression of the Thermal Effects of Ultrasound. *ACS Macro Lett.* **2012**, *1*, 1012−1015.
(27) Wang, Q.; Gossweiler, G. R.; Craig, S. L.; Zhao, X. Cephalopod-Inspired Design of Electro-Mechano-Chemically Responsive Elastomers for On-Demand Fluorescent Patterning. *Nat. Commun.* **2014**, *5*, 4899.
(28) Gossweiler, G. R.; Kouznetsova, T. B.; Craig, S. L. Force-Rate Characterization of Two Spiropyran-Based Molecular Force Probes. *J. Am. Chem. Soc.* **2015**, *137*, 6148−6151.
(29) Mullins, L. Effect of Stretching on the Properties of Rubber. *Rubber Chem. Technol.* **1948**, *21*, 281−300.
(30) Mullins, L. Softening of Rubber by Deformation. *Rubber Chem. Technol.* **1969**, *42*, 339−362.
(31) Mullins, L.; Tobin, N. R. Theoretical Model for the Elastic Behavior of Filler-Reinforced Vulcanized Rubbers. *Rubber Chem. Technol.* **1957**, *30*, 555−571.
(32) Jakobs, R. T. M.; Ma, S.; Sijbesma, R. P. Mechanocatalytic Polymerization and Cross-Linking in a Polymeric Matrix. *ACS Macro Lett.* **2013**, *2*, 613−616.
(33) Terryn, S.; Mathijssen, G.; Brancart, J.; Lefeber, D.; Assche, G. V.; Vanderborght, B. Development of a Self-Healing Soft Pneumatic Actuator: A First Concept. *Bioinspir. Biomim.* **2015**, *10*, 046007.
(34) Tolley, M. T.; Shepherd, R. F.; Mosadegh, B.; Galloway, K. C.; Wehner, M.; Karpelson, M.; Wood, R. J.; Whitesides, G. M. A Resilient, Untethered Soft Robot. *Soft Robotics* **2014**, *1*, 213−223.
(35) Kean, Z. S.; Akbulatov, S.; Tian, Y.; Widenhoefer, R. A.; Boulatov, R.; Craig, S. L. Photomechanical Actuation of Ligand Geometry in Enantioselective Catalysis. *Angew. Chem., Int. Ed.* **2014**, *53*, 14508−11.
(36) Majidi, C.; Shepherd, R. F.; Kramer, R. K.; Whitesides, G. M.; Wood, R. J. Influence of Surface Traction on Soft Robot Undulation. *Int. J. Robotics Res.* **2013**, *32*, 1577−1584.
(37) Mosadegh, B.; Polygerinos, P.; Keplinger, C.; Wennstedt, S.; Shepherd, R. F.; Gupta, U.; Shim, J.; Bertoldi, K.; Walsh, C. J.; Whitesides, G. M. Pneumatic Networks for Soft Robotics that Actuate Rapidly. *Adv. Funct. Mater.* **2014**, *24*, 2163−2170.

DOI: 10.1021/acsami.5b06440
ACS Appl. Mater. Interfaces 2015, 7, 22431−22435